Journal of Zhejiang University-SCIENCE A (Applied Physics & Engineering)
ISSN 1673-565X (Print); ISSN 1862-1775 (Online)
www.zju.edu.cn/jzus; www.springerlink.com
E-mail: jzus@zju.edu.cn

Steady-state response of a saturated half-space with an overlying dry layer subjected to a moving load

An-feng HU, Bo SUN[†‡], Kang-he XIE

(*MOE Key Laboratory of Soft Soils and Geoenvironmental Engineering, Zhejiang University, Hangzhou 310058, China*)

[†]E-mail: bosun20041016@163.com

Received July 7, 2011; Revision accepted Nov 2, 2011; Crosschecked Dec. 6, 2011

Abstract: In this paper, the steady-state response of a saturated half-space with an overlying dry layer subjected to a moving rectangular load is investigated. The governing partial differential equations are solved using the Fourier transform. The solutions in time-space domain are expressed in terms of infinite Fourier type integrals, which can be evaluated only by numerical quadrature. Numerical results show that the influence of a drained or undrained interface on the response is related to the permeability of the underlying saturated soil. Moreover, the effect due to the upper dry layer is associated with the thickness of the layer.

Key words: Steady-state response, Moving load, Saturated half-space, Overlying dry layer, Fourier transform, Drained or undrained interface

doi:10.1631/jzus.A1100184 **Document code:** A **CLC number:** TU435

1 Introduction

The study of the dynamic response of a soil medium under moving loads is of fundamental importance to several disciplines such as geotechnical engineering, seismology and transportation engineering. This problem has received wide attention over the past decades. For example, the problem of a line load moving with constant velocity over the surface of a homogeneous elastic half-space was first discussed by Sneddon (1952). He obtained the solution in a closed form, but restricted his attention only to the case of low velocities of the load. Cole and Huth (1958) considered the same problem for subsonic, transonic, and supersonic cases. The problem for a homogeneous elastic half-space subjected to a moving load was also studied by Eason (1965). Hung and Yang (2001) obtained the solutions for various loads with static and dynamic components moving on the surface of a visco-elastic half-space. Note that all the studies discussed above were about an elastic or visco-elastic soil medium.

Generally, the soil media considered are two-phase materials consisting of soil grains and pore water, and the existence of the pore fluid will affect the dynamic properties of the soil to some degree. As a result, for the analysis of the dynamic response of the soil, a saturated medium model is superior to linear elastic or visco-elastic models. The first theory of propagation of elastic waves in a fluid-saturated porous medium was established by Biot (1956; 1962). Many researchers have employed Biot's theory to study the dynamic response of a saturated medium under a moving load. For example, Burke and Kingsbury (1984) presented closed-form analytical solutions for a saturated medium subjected to traveling surface pressure. But their solutions do not account for inertia forces which are considered in Biot's theory and are applicable only to a single layer. The dynamic response of a saturated half-space to moving loads under plane-strain conditions was presented by Siddharthan *et al.* (1993).

‡ Corresponding author

However, the relative motion between the solid and fluid was neglected in their solutions. Theodorakopoulos (2003), considering this relative movement, discussed the dynamic response of a saturated half-plane under moving line loads. Lu and Jeng (2007) considered the dynamic response of a saturated half-space subjected to a moving point load. Jin *et al.* (2004) and Bo (2004) examined the stresses and excess pore fluid pressure that are induced in a saturated half-space under a concentrated line load. Cai *et al.* (2007) presented the steady-state responses of a saturated half-space soil medium to a moving rectangular load. The ground vibration due to a high-speed moving vertical harmonic rectangular load was investigated theoretically by Lefeuve-Mesgouez and Mesgouez (2008). They discussed not only the fully saturated half-space but also the partially saturated ground. For a partially saturated ground, a third phase (gas phase) has been taken into account. The connected porosity is filled with both liquid and gas phases (the gas phase forms small bubbles mixed in the liquid phase). Xu *et al.* (2008) proposed a 3D analytical solution for the dynamic response of a saturated multi-layered half-space subjected to a moving point load applied on the ground surface.

In all of those studies, the medium was homogeneous (saturated or partially saturated up to the free surface). In practice, however, the underground water level is usually several meters beneath the free surface. To consider this effect, the present study introduces saturation at certain depths below the free surface. The half-space is divided into two layers: an upper thin dry layer is modeled by elastic medium and the underlying saturated half-space is considered as a two-phase medium that follows Biot (1956)'s theory. In addition, the interface between the upper dry layer and the bottom saturated half-space is considered to be either drained (all stresses from the layer are transmitted to the skeleton of the bottom half-space at the interface while the pore fluid pressure is zero) or undrained (stresses from the layer are transmitted to both solid and fluid constituents of the bottom half-space at the interface, and thus the pore fluid pressure is not zero). Thus, the present model is entirely different to models of fully saturated or partially saturated media.

In this paper, we propose a 3D semi-analytical approach to study the dynamic response of a saturated half-space with an upper dry layer induced by a moving rectangular load. The governing partial differential equations are solved using the Fourier transform. Using the boundary conditions on the free surface of the upper dry layer and the continuity conditions across the interface, explicit analytical solutions in the transformed domain are established. The solutions in time-space domain are expressed in terms of infinite Fourier type integrals, which can be evaluated only by numerical quadrature. When reduced to some special cases, our solutions agree very well with the known results.

This paper concentrated on investigating the effect of the overlying dry layer on the dynamic response. The influence of the permeability of the interface (i.e., a drained or undrained interface) is also studied.

Note that all the studies mentioned above (including this study) are about steady-state response. It is assumed that the load has been moving for a considerable length of time so that all transient disturbances produced at the initial point of application have died out leaving only a steady pattern of response.

2 Governing equations and general solutions

The constitutive relations for a homogeneous saturated medium based on Biot (1956)'s theory can be expressed as

$$\sigma_{ij} = \lambda\delta_{ij}\theta + \mu(u_{i,j} + u_{j,i}) - \alpha\delta_{ij}p, \tag{1}$$

$$p = -\alpha M\theta + M\zeta, \tag{2}$$

where the subscripts $(\ )_{,i}$ denote spatial derivatives; σ_{ij} is the total stress of the bulk material and p is the excess pore fluid pressure (suction is considered negative); θ=$u_{i,j}$ is the dilatation of the solid skeleton; ζ=$-w_{i,j}$ is the volume of fluid injection into a unit volume of the bulk material; δ_{ij} is the Kronecher delta; λ and μ are Lame constants; and α and M are Biot's parameters accounting for compressibility of the two-phase material.

The equations of motion of a homogeneous saturated medium can be written in terms of the displacements u_i and w_i as (Biot, 1956)

$$\mu u_{i,jj}+(\lambda+\alpha^2M+\mu)u_{j,ji}+\alpha M w_{j,ji}=\rho\ddot{u}_i+\rho_{\mathrm{f}}\ddot{w}_i, \quad (3)$$

$$\alpha M u_{j,ji}+M w_{j,ji}=\rho_{\mathrm{f}}\ddot{u}_i+m\ddot{w}_i+\frac{1}{k}\dot{w}_i, \quad (4)$$

where u_i and w_i denote the average solid displacement and the pore fluid displacement relative to the solid matrix in the i-direction (i=x, y, z) respectively; The dot over a variable denotes the time derivative; ρ and ρ_{f} are the mass densities of the bulk material and the pore fluid, respectively; $\rho=n\rho_{\mathrm{f}}+(1-n)\rho_{\mathrm{s}}$, ρ_{s} is the density of the solid skeleton and n is the porosity of the porous medium; and m is the density-like parameter that depends on ρ_{f} and the geometry of the pores. The parameter k is the hydraulic permeability coefficient, which accounts for the internal viscous friction derived from the relative motion between the solid skeleton and the pore fluid.

The preceding equations can be reduced to a simple set of equations through the use of the Helmholtz potential. Let the displacement fields u_i and w_i be represented as

$$u_i=\mathrm{grad}\phi_1+\mathrm{curl}\varphi_j, \quad (5a)$$

$$w_i=\mathrm{grad}\phi_2+\mathrm{curl}\Phi_j, \quad (5b)$$

where ϕ_1 and φ_j (j=1, 2) are the scalar and vector potentials for the solid displacements, while ϕ_2 and Φ_j (j=1, 2) are those for the pore fluid.

Substituting Eq. (5) into Eqs. (3) and (4) yields:

$$\left((\lambda+\alpha^2M+2\mu)\nabla^2-\rho\frac{\partial^2}{\partial t^2}\right)\phi_1=-\left(\alpha M\nabla^2-\rho_{\mathrm{f}}\frac{\partial^2}{\partial t^2}\right)\phi_2, \quad (6a)$$

$$\left(\alpha M\nabla^2-\rho_{\mathrm{f}}\frac{\partial^2}{\partial t^2}\right)\phi_1=-\left(M\nabla^2-m\frac{\partial^2}{\partial t^2}-\frac{1}{k}\frac{\partial}{\partial t}\right)\phi_2, \quad (6b)$$

$$\left(\nabla^2-\frac{\rho\partial^2}{\mu\partial t^2}\right)\varphi_1=\frac{\rho_{\mathrm{f}}\partial^2}{\mu\partial t^2}\Phi_1, \quad (6c)$$

$$-\rho_{\mathrm{f}}\frac{\partial^2}{\partial t^2}\varphi_1=\left(m\frac{\partial^2}{\partial t^2}+\frac{1}{k}\frac{\partial}{\partial t}\right)\Phi_1, \quad (6d)$$

$$\left(\nabla^2-\frac{\rho\partial^2}{\mu\partial t^2}\right)\varphi_2=\frac{\rho_{\mathrm{f}}}{\mu}\frac{\partial^2}{\partial t^2}\Phi_2, \quad (6e)$$

$$-\rho_{\mathrm{f}}\frac{\partial^2}{\partial t^2}\varphi_2=\left(m\frac{\partial^2}{\partial t^2}+\frac{1}{k}\frac{\partial}{\partial t}\right)\Phi_2, \quad (6f)$$

where ∇^2 is the Laplacian operator defined by $\nabla^2=\frac{\partial^2}{\partial x^2}+\frac{\partial^2}{\partial y^2}+\frac{\partial^2}{\partial z^2}$.

In this study, the triple Fourier transform of function $f(x, y, z, t)$ with respect to time and two horizontal coordinates is defined as follows:

$$\begin{aligned}&\hat{\bar{f}}(\xi,\eta,z,\omega)\\&=\int_{-\infty}^{\infty}\int_{-\infty}^{\infty}\int_{-\infty}^{\infty}f(x,y,z,t)\mathrm{e}^{-\mathrm{i}\xi x}\mathrm{e}^{-\mathrm{i}\eta y}\mathrm{e}^{-\mathrm{i}\omega t}\mathrm{d}x\mathrm{d}y\mathrm{d}t,\end{aligned} \quad (7a)$$

and the inverse relationship is given by

$$\begin{aligned}&f(x,y,z,t)\\&=\frac{1}{(2\pi)^3}\int_{-\infty}^{\infty}\int_{-\infty}^{\infty}\int_{-\infty}^{\infty}\hat{\bar{f}}(\xi,\eta,z,\omega)\mathrm{e}^{\mathrm{i}\xi x}\mathrm{e}^{\mathrm{i}\eta y}\mathrm{e}^{\mathrm{i}\omega t}\mathrm{d}\xi\mathrm{d}\eta\mathrm{d}\omega,\end{aligned} \quad (7b)$$

where ω, ξ and η represent frequency and the two horizontal wave numbers corresponding to x and y directions, respectively. The superimposed symbol "^" above the variable denotes the Fourier transform with respect to time t, and the double "¯" denotes the Fourier transform with respect to x and y coordinates.

Performing the triple Fourier transformation on Eq. (6), the original partial differential equations are changed to ordinary differential equations with the vertical coordinate z serving as the variable. In Eqs. (1)–(5), the general solutions in the transformed domain (frequency-wavenumber domain) for displacements u_i and w_i (i=x, y, z), stresses σ_{ij} (i, j=x, y, z) and pore fluid pressure p can be expressed as

$$\left[\mathrm{i}\hat{\bar{u}}_x\ \ \mathrm{i}\hat{\bar{u}}_y\ \ \hat{\bar{u}}_z\ \ \hat{\bar{w}}_z\ \ \mathrm{i}\hat{\bar{\sigma}}_{xz}\ \ \mathrm{i}\hat{\bar{\sigma}}_{yz}\ \ \hat{\bar{\sigma}}_{zz}\ \ \hat{\bar{p}}\right]^{\mathrm{T}}=\boldsymbol{R}(z)\boldsymbol{\Delta}, \quad (8)$$

where $\boldsymbol{\Delta}=[A\ B\ C\ D\ E\ F\ G\ H]^{\mathrm{T}}$, in which $A(\xi, \eta, \omega)$, $B(\xi, \eta, \omega)$, $C(\xi, \eta, \omega)$, $D(\xi, \eta, \omega)$, $E(\xi, \eta, \omega)$, $F(\xi, \eta, \omega)$, $G(\xi, \eta, \omega)$, and $H(\xi, \eta, \omega)$ are arbitrary constants to be determined by using the corresponding boundary and continuity conditions relevant to a given problem and

$$\boldsymbol{R}(z)=\begin{bmatrix}
-\xi \mathrm{e}^{r_1 z} & -\xi \mathrm{e}^{-r_1 z} & -\xi \mathrm{e}^{r_2 z} & -\xi \mathrm{e}^{-r_2 z} & 0 & 0 & -\mathrm{i}r_3 \mathrm{e}^{r_3 z} & \mathrm{i}r_3 \mathrm{e}^{-r_3 z} \\
-\eta \mathrm{e}^{r_1 z} & -\eta \mathrm{e}^{-r_1 z} & -\eta \mathrm{e}^{r_2 z} & -\eta \mathrm{e}^{-r_2 z} & \mathrm{i}r_3 \mathrm{e}^{r_3 z} & -\mathrm{i}r_3 \mathrm{e}^{-r_3 z} & 0 & 0 \\
r_1 \mathrm{e}^{r_1 z} & -r_1 \mathrm{e}^{-r_1 z} & r_2 \mathrm{e}^{r_2 z} & -r_2 \mathrm{e}^{-r_2 z} & -\mathrm{i}\eta \mathrm{e}^{r_3 z} & -\mathrm{i}\eta \mathrm{e}^{-r_3 z} & \mathrm{i}\xi \mathrm{e}^{r_3 z} & \mathrm{i}\xi \mathrm{e}^{-r_3 z} \\
r_1\chi_1 \mathrm{e}^{r_1 z} & -r_1\chi_1 \mathrm{e}^{-r_1 z} & r_2\chi_2 \mathrm{e}^{r_2 z} & -r_2\chi_2 \mathrm{e}^{-r_2 z} & -\mathrm{i}\eta\chi_3 \mathrm{e}^{r_3 z} & -\mathrm{i}\eta\chi_3 \mathrm{e}^{-r_3 z} & \mathrm{i}\xi\chi_3 \mathrm{e}^{r_3 z} & \mathrm{i}\xi\chi_3 \mathrm{e}^{-r_3 z} \\
-2\mu\xi r_1 \mathrm{e}^{r_1 z} & 2\mu\xi r_1 \mathrm{e}^{-r_1 z} & -2\mu\xi r_2 \mathrm{e}^{r_2 z} & 2\mu\xi r_2\ \mathrm{e}^{-r_2 z} & \mathrm{i}\mu\xi\eta \mathrm{e}^{r_3 z} & \mathrm{i}\mu\xi\eta \mathrm{e}^{-r_3 z} & -\mathrm{i}a_3 \mathrm{e}^{r_3 z} & -\mathrm{i}a_3 \mathrm{e}^{-r_3 z} \\
-2\mu\eta r_1 \mathrm{e}^{r_1 z} & 2\mu\eta r_1 \mathrm{e}^{-r_1 z} & -2\mu\eta r_2 \mathrm{e}^{r_2 z} & 2\mu\eta r_2 \mathrm{e}^{-r_2 z} & \mathrm{i}b_3 \mathrm{e}^{r_3 z} & \mathrm{i}b_3 \mathrm{e}^{-r_3 z} & -\mathrm{i}\mu\xi\eta \mathrm{e}^{r_3 z} & -\mathrm{i}\mu\xi\eta \mathrm{e}^{-r_3 z} \\
c_1 \mathrm{e}^{r_1 z} & c_1 \mathrm{e}^{-r_1 z} & c_2 \mathrm{e}^{r_2 z} & c_2 \mathrm{e}^{-r_2 z} & -2\mathrm{i}\mu\eta r_3 \mathrm{e}^{r_3 z} & 2\mathrm{i}\mu\eta r_3 \mathrm{e}^{-r_3 z} & 2\mathrm{i}\mu\xi r_3 \mathrm{e}^{r_3 z} & -2\mathrm{i}\mu\xi r_3 \mathrm{e}^{-r_3 z} \\
a_1 \mathrm{e}^{r_1 z} & a_1 \mathrm{e}^{-r_1 z} & a_2 \mathrm{e}^{r_2 z} & a_2 \mathrm{e}^{-r_2 z} & 0 & 0 & 0 & 0
\end{bmatrix}, \quad (9)$$

where

$$\chi_i=\frac{-(\lambda+2\mu)L_i^2+\rho\omega^2-\alpha\rho_\mathrm{f}\omega^2}{-\rho_\mathrm{f}\omega^2+\alpha m\omega^2-\dfrac{\alpha\omega\mathrm{i}}{k}},\ i=1,2,$$

$$\chi_3=\frac{\rho_\mathrm{f}\omega^2}{\dfrac{\mathrm{i}\omega}{k}-m\omega^2},$$

$$a_i=(\alpha+\chi_i)ML_i^2, i=1,2$$

$$a_3=\mu(\xi^2+r_3^2),$$

$$b_3=\mu(\eta^2+r_3^2),$$

$$c_i=2\mu r_i^2-\lambda L_i^2-\alpha a_i,\ i=1,2,$$

$$r_i=\sqrt{\xi^2+\eta^2-L_i^2},\ i=1,2,$$

$$r_3=\sqrt{\xi^2+\eta^2-S^2},$$

$$L_1^2=\frac{\beta_1+\sqrt{\beta_1^2-4\beta_2}}{2},$$

$$L_2^2=\frac{\beta_1-\sqrt{\beta_1^2-4\beta_2}}{2},$$

$$S^2=\frac{(\rho_\mathrm{f}\chi_3+\rho)\omega^2}{\mu},$$

$$\beta_1=\frac{\left(m\omega^2-\dfrac{\mathrm{i}\omega}{k}\right)(\lambda+\alpha^2M+2\mu)+\rho\omega^2M-2\alpha\rho_\mathrm{f}\omega^2M}{(\lambda+2\mu)M},$$

$$\beta_2=\frac{\left(m\omega^2-\dfrac{\mathrm{i}\omega}{k}\right)\rho\omega^2-\rho_\mathrm{f}^2\omega^4}{(\lambda+2\mu)M},$$

where L_1, L_2 and S are the complex wave numbers associated with the dilatational wave of the first kind, the dilatational wave of the second kind and the rotational wave, respectively (Biot, 1956). Note that the radicals r_i (i=1, 2, 3) are selected such that Re(r_i)≥0. Further, columns one and two in the right-hand side of Eq. (9) belong to the P1 (fast compressional) mode, three and four to the P2 (slow compressional) mode, five and six to the SV-mode and seven and eight to the SH-mode of the saturated soil.

In the limiting case of $M=\rho_\mathrm{f}=m=\dfrac{1}{k}=\alpha=0$, the general solutions for a elastic medium can be easily deduced from Eq. (8):

$$\left[\mathrm{i}\hat{\bar{u}}_x^\mathrm{e}\quad \mathrm{i}\hat{\bar{u}}_y^\mathrm{e}\quad \hat{\bar{u}}_z^\mathrm{e}\quad \mathrm{i}\hat{\bar{\sigma}}_{xz}^\mathrm{e}\quad \mathrm{i}\hat{\bar{\sigma}}_{yz}^\mathrm{e}\quad \hat{\bar{\sigma}}_{zz}^\mathrm{e}\right]^\mathrm{T}=\boldsymbol{R}^\mathrm{e}(z)\boldsymbol{\Delta}^\mathrm{e}, \quad (10)$$

where u_i^e and σ_{ij}^e (i,j=x, y, z) denote the displacement and total stress of the elastic medium, respectively; $\boldsymbol{\Delta}^\mathrm{e}$=$[A_1\ B_1\ C_1\ D_1\ E_1\ F_1\ G_1\ H_1]^\mathrm{T}$, in which $A_1(\xi, \eta, \omega)$, $B_1(\xi, \eta, \omega)$, $C_1(\xi, \eta, \omega)$, $D_1(\xi, \eta, \omega)$, $E_1(\xi, \eta, \omega)$, $F_1(\xi, \eta, \omega)$ are the constants to be determined; the superscript "e" denotes the upper elastic layer and $\boldsymbol{R}^\mathrm{e}(z)$ can be expressed by Eq. (11) as shown in the next page, where

$$r_4=\sqrt{\xi^2+\eta^2-\frac{\rho^\mathrm{e}\omega^2}{\lambda^\mathrm{e}+2\mu^\mathrm{e}}};\qquad r_5=\sqrt{\xi^2+\eta^2-\frac{\rho^\mathrm{e}\omega^2}{\mu^\mathrm{e}}};$$

a_4=$(\xi^2$+$r_5^2)\mu^\mathrm{e}$; b_4=$(\eta^2$+$r_5^2)\mu^\mathrm{e}$; and c_4=$(\lambda^\mathrm{e}$+$2\mu^\mathrm{e})r_4^2$−$\lambda^\mathrm{e}(\xi^2$+$\eta^2)$. Similarly, as mentioned above, the radicals r_i (i=4, 5) are selected such that Re(r_i)≥0 and columns one and two in the right-hand side of Eq. (11) belong to the P-mode, three and four to the SV-mode, and five and six to the SH-mode of the elastic medium.

$$\boldsymbol{R}^{\mathrm{e}}(z)=\begin{bmatrix} -\xi \mathrm{e}^{r_4 z} & -\xi \mathrm{e}^{-r_4 z} & 0 & 0 & -\mathrm{i}r_5 \mathrm{e}^{r_5 z} & \mathrm{i}r_5 \mathrm{e}^{-r_5 z} \\ -\eta \mathrm{e}^{r_4 z} & -\eta \mathrm{e}^{-r_4 z} & \mathrm{i}r_5 \mathrm{e}^{r_5 z} & -\mathrm{i}r_5 \mathrm{e}^{-r_5 z} & 0 & 0 \\ r_4 \mathrm{e}^{r_4 z} & -r_4 \mathrm{e}^{-r_4 z} & -\mathrm{i}\eta \mathrm{e}^{r_5 z} & -\mathrm{i}\eta \mathrm{e}^{-r_5 z} & \mathrm{i}\xi \mathrm{e}^{r_5 z} & \mathrm{i}\xi \mathrm{e}^{-r_5 z} \\ -2\mu^{\mathrm{e}}\xi r_4 \mathrm{e}^{r_4 z} & 2\mu^{\mathrm{e}}\xi r_4 \mathrm{e}^{-r_4 z} & \mathrm{i}\mu^{\mathrm{e}}\xi\eta \mathrm{e}^{r_5 z} & \mathrm{i}\mu^{\mathrm{e}}\xi\eta \mathrm{e}^{-r_5 z} & -\mathrm{i}a_4 \mathrm{e}^{r_5 z} & -\mathrm{i}a_4 \mathrm{e}^{-r_5 z} \\ -2\mu^{\mathrm{e}}\eta r_4 \mathrm{e}^{r_4 z} & 2\mu^{\mathrm{e}}\eta r_4 \mathrm{e}^{-r_4 z} & \mathrm{i}b_4 \mathrm{e}^{r_5 z} & \mathrm{i}b_4 \mathrm{e}^{-r_5 z} & -\mathrm{i}\mu^{\mathrm{e}}\xi\eta \mathrm{e}^{r_5 z} & -\mathrm{i}\mu^{\mathrm{e}}\xi\eta \mathrm{e}^{-r_5 z} \\ c_4 \mathrm{e}^{r_4 z} & c_4 \mathrm{e}^{-r_4 z} & -2\mathrm{i}\mu^{\mathrm{e}}\eta r_5 \mathrm{e}^{r_5 z} & 2\mathrm{i}\mu^{\mathrm{e}}\eta r_5 \mathrm{e}^{-r_5 z} & 2\mathrm{i}\mu^{\mathrm{e}}\xi r_5 \mathrm{e}^{r_5 z} & -2\mathrm{i}\mu^{\mathrm{e}}\xi r_5 \mathrm{e}^{-r_5 z} \end{bmatrix}. \quad (11)$$

In addition, λ^{e} and μ^{e} are Lame constants and ρ^{e} is the density of the elastic medium. Note that the soil skeleton of the upper dry layer is the same as that of the underlying saturated half-space. As a result, the parameter $\lambda^{\mathrm{e}}=\lambda$, $\mu^{\mathrm{e}}=\mu$ and $\rho^{\mathrm{e}}=(1-n)\rho_{\mathrm{s}}$. The corresponding compression and shear wave speeds in the elastic medium, c_{p} and c_{s} respectively, are defined as

$$c_{\mathrm{p}}=\sqrt{\frac{\lambda^{\mathrm{e}}+2\mu^{\mathrm{e}}}{\rho^{e}}},\quad c_{\mathrm{s}}=\sqrt{\frac{\mu^{\mathrm{e}}}{\rho^{\mathrm{e}}}}.$$

3 Boundary and continuity conditions

The model with an elastic layer overlying the saturated half-space considered herein is illustrated in Fig. 1. The thickness of the elastic layer is h_1. A moving vertical load acts uniformly over a rectangle with dimensions $2a\times 2b$. It moves over the surface of the upper elastic layer with constant velocity c along the positive x direction. The boundary and continuity conditions corresponding to this saturated half-space with an overlying dry layer can be expressed as (Xu *et al*., 2008)

$$\sigma_{xz}^{\mathrm{e}}(x,y,0)=0, \quad (12a)$$

$$\sigma_{yz}^{\mathrm{e}}(x,y,0)=0, \quad (12b)$$

$$\sigma_{zz}^{\mathrm{e}}(x,y,0)=-f_0 H[a^2-(x-ct)^2]H[b^2-y^2], \quad (12c)$$

$$u_x^{\mathrm{e}}(x,y,h_1)-u_x^{\mathrm{s}}(x,y,h_1)=0, \quad (12d)$$

$$u_y^{\mathrm{e}}(x,y,h_1)-u_y^{\mathrm{s}}(x,y,h_1)=0, \quad (12e)$$

$$u_z^{\mathrm{e}}(x,y,h_1)-u_z^{\mathrm{e}}(x,y,h_1)=0, \quad (12f)$$

$$\sigma_{xz}^{\mathrm{e}}(x,y,h_1)-\sigma_{xz}^{\mathrm{s}}(x,y,h_1)=0, \quad (12g)$$

$$\sigma_{yz}^{\mathrm{e}}(x,y,h_1)-\sigma_{yz}^{\mathrm{s}}(x,y,h_1)=0, \quad (12h)$$

$$\sigma_{zz}^{\mathrm{e}}(x,y,h_1)-\sigma_{zz}^{\mathrm{s}}(x,y,h_1)=0, \quad (12i)$$

where the superscript "s" denotes the underlying half-space, f_0 is the intensity of the uniformly distributed load, and $H[]$ denotes the Heaviside step function, which is defined as

$$H[\vartheta]=\begin{cases}1, & \vartheta>0,\\ 0, & \vartheta<0.\end{cases} \quad (13)$$

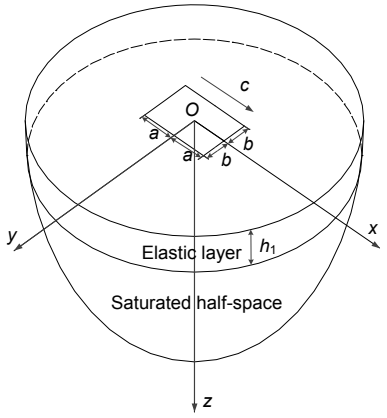

Fig. 1 A saturated half-space with an overlying dry layer subjected to a moving rectangular load

Another equation can be obtained by considering the interface as pervious or impervious. For the case of a pervious interface, the pore fluid pressure is zero at the interface, while for the case of an impervious interface, the vertical displacement of the fluid is assumed to be zero at the interface. Hereinafter, the above two cases will be referred to as the drained or undrained interface, respectively. Thus, the two cases considered can be expressed as (Theodorakopoulos, 2003)

For the drained interface:

$$p^{\mathrm{s}}(x,y,h_1)=0; \quad (14a)$$

For the undrained interface:

$$w_z^s(x,y,h_1)=0. \tag{14b}$$

According to Eq. (14a), all stresses from the layer are transmitted to the skeleton of the bottom half-space at the interface in the drained case. In the case of the undrained interface (Eq. (14b)), stresses from the layer are transmitted to both the solid and fluid constituents of the bottom half-space at the interface, and thus the pore fluid pressure is not zero.

Because of the radiation condition imposed for the half-space at infinity, the four exponentially increasing terms of the underlying saturated half-space will be discarded (i.e., $A=C=E=G=0$).

Note that, in total, the numbers of the boundary and continuity conditions are equal to the numbers of the unknowns for the saturated half-space with an overlying dry layer. Therefore, the solutions for constants B, D, E, H and $A_1, B_1, C_1, D_1, E_1, F_1$ are possible in principle.

4 Solutions for a saturated half-space with an overlying dry layer

Fourier transformations of the boundary and continuity conditions are given by Eqs. (12) and (14), after some manipulations, and the following system of algebraic equations is obtained:

$$\boldsymbol{K}_1\boldsymbol{v}=\boldsymbol{f}, \tag{15a}$$

where $\boldsymbol{v}$ denotes an unknown vector of wave-field amplitudes given by

$$\begin{aligned}\boldsymbol{v}^{\mathrm{T}}=[&A_1\mathrm{e}^{h_1r_4}\ \ B_1\mathrm{e}^{-h_1r_4}\ \ C_1\mathrm{e}^{h_1r_5}\ \ D_1\mathrm{e}^{-h_1r_5}\ \ E_1\mathrm{e}^{h_1r_5}\\ &F_1\mathrm{e}^{-h_1r_5}\ \ B\mathrm{e}^{-h_1r_1}\ \ D\mathrm{e}^{-h_1r_2}\ \ F\mathrm{e}^{-h_1r_3}\ \ H\mathrm{e}^{-h_1r_3}],\end{aligned} \tag{15b}$$

and

$$\boldsymbol{f}^{\mathrm{T}}=\left[0\ \ 0\ \ -\hat{\hat{\bar{F}}}\ \ 0\ \ 0\ \ 0\ \ 0\ \ 0\ \ 0\ \ 0\right], \tag{15c}$$

where $\hat{\hat{\bar{F}}}$ is the Fourier form of the moving load. According to Eq. (12c), we know that $F=f_0H[a^2-(x-ct)^2]H[b^2-y^2]$, thus $\hat{\hat{\bar{F}}}=8\pi f_0\dfrac{\sin(\xi a)}{\xi}\dfrac{\sin(\eta b)}{\eta}\delta(\omega+c\xi)$ in which $\delta()$ is Dirac's delta function.

In addition, the 10×10 complex non-symmetric matrix $\boldsymbol{K}_1$ is expressed by Eq. (15d) as below.

Note that the matrix $\boldsymbol{K}_1$ is associated with the drained condition at the interface $z=h_1$. In the case of the undrained interface, the corresponding equation is given as

$$\boldsymbol{K}_2\boldsymbol{v}=\boldsymbol{f}, \tag{16a}$$

where $\boldsymbol{K}_2$ is expressed by Eq. (16b) as shown in the next page.

$$\boldsymbol{K}_1=\begin{bmatrix}
-2\mu^{\mathrm{e}}\xi r_4\mathrm{e}^{-h_1r_4} & 2\mu^{\mathrm{e}}\xi r_4\mathrm{e}^{h_1r_4} & \mathrm{i}\mu^{\mathrm{e}}\xi\eta\mathrm{e}^{-h_1r_5} & \mathrm{i}\mu^{\mathrm{e}}\xi\eta\mathrm{e}^{h_1r_5} & -\mathrm{i}a_4\mathrm{e}^{-h_1r_5} & -\mathrm{i}a_4\mathrm{e}^{h_1r_5} & 0 & 0 & 0 & 0\\
-2\mu^{\mathrm{e}}\eta r_4\mathrm{e}^{-h_1r_4} & 2\mu^{\mathrm{e}}\eta r_4\mathrm{e}^{h_1r_4} & \mathrm{i}b_4\mathrm{e}^{-h_1r_5} & \mathrm{i}b_4\mathrm{e}^{h_1r_5} & -\mathrm{i}\mu^{\mathrm{e}}\xi\eta\mathrm{e}^{-h_1r_5} & -\mathrm{i}\mu^{\mathrm{e}}\xi\eta\mathrm{e}^{h_1r_5} & 0 & 0 & 0 & 0\\
c_4\mathrm{e}^{-h_1\gamma_4} & c_4\mathrm{e}^{h_1\gamma_4} & -2\mathrm{i}\mu^{\mathrm{e}}\eta\gamma_5\mathrm{e}^{-h_1\gamma_5} & 2\mathrm{i}\mu^{\mathrm{e}}\eta\gamma_5\mathrm{e}^{h_1\gamma_5} & 2\mathrm{i}\mu^{\mathrm{e}}\xi\gamma_5\mathrm{e}^{-h_1\gamma_5} & -2\mathrm{i}\mu^{\mathrm{e}}\xi\gamma_5\mathrm{e}^{h_1\gamma_5} & 0 & 0 & 0 & 0\\
-\xi & -\xi & 0 & 0 & -\mathrm{i}\gamma_5 & \mathrm{i}\gamma_5 & \xi & \xi & 0 & -\mathrm{i}\gamma_3\\
-\eta & -\eta & \mathrm{i}\gamma_5 & -\mathrm{i}\gamma_5 & 0 & 0 & \eta & \eta & \mathrm{i}\gamma_3 & 0\\
\gamma_4 & -\gamma_4 & -\mathrm{i}\eta & -\mathrm{i}\eta & \mathrm{i}\xi & \mathrm{i}\xi & \gamma_1 & \gamma_2 & \mathrm{i}\eta & -\mathrm{i}\xi\\
-2\mu^{\mathrm{e}}\xi\gamma_4 & 2\mu^{\mathrm{e}}\xi\gamma_4 & \mathrm{i}\mu^{\mathrm{e}}\xi\eta & \mathrm{i}\mu^{\mathrm{e}}\xi\eta & -\mathrm{i}a_4 & -\mathrm{i}a_4 & -2\mu\xi\gamma_1 & -2\mu\xi\gamma_2 & -\mathrm{i}\mu\xi\eta & \mathrm{i}a_3\\
-2\mu^{\mathrm{e}}\eta\gamma_4 & 2\mu^{\mathrm{e}}\eta\gamma_4 & \mathrm{i}b_4 & \mathrm{i}b_4 & -\mathrm{i}\mu^{\mathrm{e}}\xi\eta & -\mathrm{i}\mu^{\mathrm{e}}\xi\eta & -2\mu\eta\gamma_1 & -2\mu\eta\gamma_2 & -\mathrm{i}b_3 & \mathrm{i}\mu\xi\eta\\
c_4 & c_4 & -2\mathrm{i}\mu^{\mathrm{e}}\eta\gamma_5 & 2\mathrm{i}\mu^{\mathrm{e}}\eta\gamma_5 & 2\mathrm{i}\mu^{\mathrm{e}}\xi\gamma_5 & -2\mathrm{i}\mu^{\mathrm{e}}\xi\gamma_5 & -c_1 & -c_2 & -2\mathrm{i}\mu\eta\gamma_3 & 2\mathrm{i}\mu\xi\gamma_3\\
0 & 0 & 0 & 0 & 0 & 0 & a_1 & a_2 & 0 & 0
\end{bmatrix}, \tag{15d}$$

$$\boldsymbol{K}_2=\begin{bmatrix}
-2\mu^{\mathrm{e}}\xi r_4\mathrm{e}^{-h_1 r_4} & 2\mu^{\mathrm{e}}\xi r_4\mathrm{e}^{h_1 r_4} & \mathrm{i}\mu^{\mathrm{e}}\xi\eta\mathrm{e}^{-h_1 r_5} & \mathrm{i}\mu^{\mathrm{e}}\xi\eta\mathrm{e}^{h_1 r_5} & -\mathrm{i}a_4\mathrm{e}^{-h_1 r_5} & -\mathrm{i}a_4\mathrm{e}^{h_1 r_5} & 0 & 0 & 0 & 0\\
-2\mu^{\mathrm{e}}\eta r_4\mathrm{e}^{-h_1 r_4} & 2\mu^{\mathrm{e}}\eta r_4\mathrm{e}^{h_1 r_4} & \mathrm{i}b_4\mathrm{e}^{-h_1 r_5} & \mathrm{i}b_4\mathrm{e}^{h_1 r_5} & -\mathrm{i}\mu^{\mathrm{e}}\xi\eta\mathrm{e}^{-h_1 r_5} & -\mathrm{i}\mu^{\mathrm{e}}\xi\eta\mathrm{e}^{h_1 r_5} & 0 & 0 & 0 & 0\\
c_4\mathrm{e}^{-h_1\gamma_4} & c_4\mathrm{e}^{h_1\gamma_4} & -2\mathrm{i}\mu^{\mathrm{e}}\eta\gamma_5\mathrm{e}^{-h_1\gamma_5} & 2\mathrm{i}\mu^{\mathrm{e}}\eta\gamma_5\mathrm{e}^{h_1\gamma_5} & 2\mathrm{i}\mu^{\mathrm{e}}\xi\gamma_5\mathrm{e}^{-h_1\gamma_5} & -2\mathrm{i}\mu^{\mathrm{e}}\xi\gamma_5\mathrm{e}^{h_1\gamma_5} & 0 & 0 & 0 & 0\\
-\xi & -\xi & 0 & 0 & -\mathrm{i}\gamma_5 & \mathrm{i}\gamma_5 & \xi & \xi & 0 & -\mathrm{i}\gamma_3\\
-\eta & -\eta & \mathrm{i}\gamma_5 & -\mathrm{i}\gamma_5 & 0 & 0 & \eta & \eta & \mathrm{i}\gamma_3 & 0\\
\gamma_4 & -\gamma_4 & -\mathrm{i}\eta & -\mathrm{i}\eta & \mathrm{i}\xi & \mathrm{i}\xi & \gamma_1 & \gamma_2 & \mathrm{i}\eta & -\mathrm{i}\xi\\
-2\mu^{\mathrm{e}}\xi\gamma_4 & 2\mu^{\mathrm{e}}\xi\gamma_4 & \mathrm{i}\mu^{\mathrm{e}}\xi\eta & \mathrm{i}\mu^{\mathrm{e}}\xi\eta & -\mathrm{i}a_4 & -\mathrm{i}a_4 & -2\mu\xi\gamma_1 & -2\mu\xi\gamma_2 & -\mathrm{i}\mu\xi\eta & \mathrm{i}a_3\\
-2\mu^{\mathrm{e}}\eta\gamma_4 & 2\mu^{\mathrm{e}}\eta\gamma_4 & \mathrm{i}b_4 & \mathrm{i}b_4 & -\mathrm{i}\mu^{\mathrm{e}}\xi\eta & -\mathrm{i}\mu^{\mathrm{e}}\xi\eta & -2\mu\eta\gamma_1 & -2\mu\eta\gamma_2 & -\mathrm{i}b_3 & \mathrm{i}\mu\xi\eta\\
c_4 & c_4 & -2\mathrm{i}\mu^{\mathrm{e}}\eta\gamma_5 & 2\mathrm{i}\mu^{\mathrm{e}}\eta\gamma_5 & 2\mathrm{i}\mu^{\mathrm{e}}\xi\gamma_5 & -2\mathrm{i}\mu^{\mathrm{e}}\xi\gamma_5 & -c_1 & -c_2 & -2\mathrm{i}\mu\eta\gamma_3 & 2\mathrm{i}\mu\xi\gamma_3\\
0 & 0 & 0 & 0 & 0 & 0 & -\gamma_1\chi_1 & -\gamma_2\chi_2 & -\mathrm{i}\eta\chi_3 & \mathrm{i}\xi\chi_3
\end{bmatrix}. \tag{16b}$$

The constants B, D, F, H and A_1, B_1, C_1, D_1, E_1, F_1 can be deduced from the two given systems of algebraic equations (Eqs. (15a) and (16a)):

Drained case:

$$\boldsymbol{v}=\boldsymbol{K}_1^{-1}\boldsymbol{f}; \tag{17a}$$

Undrained case:

$$\boldsymbol{v}=\boldsymbol{K}_2^{-1}\boldsymbol{f}, \tag{17b}$$

where $\boldsymbol{K}_1^{-1}$ and $\boldsymbol{K}_2^{-1}$ denote the inverse matrices of $\boldsymbol{K}_1$ and $\boldsymbol{K}_2$, respectively.

After the vector $\boldsymbol{v}$ is determined, the displacements, stresses and pore fluid pressures in the transformed domain (frequency-wavenumber domain) can be determined by Eqs. (8) and (10).

In the limiting case of h_1=0, the solutions for a homogeneous saturated half-space under a moving load are obtained simply.

The final solutions in time-space domain can be obtained by performing the triple inverse Fourier transform. For simplicity, the solutions are presented in a uniform form:

$$\Omega(x,y,z,t)=\frac{f_0}{(2\pi)^3}\times\int_{-\infty}^{\infty}\int_{-\infty}^{\infty}\int_{-\infty}^{\infty}\delta(\omega+c\xi)\hat{\hat{\bar{\Omega}}}(\xi,\eta,\omega,z)\mathrm{e}^{\mathrm{i}\xi x}\mathrm{e}^{\mathrm{i}\omega t}\mathrm{e}^{\mathrm{i}\eta y}\mathrm{d}\xi\mathrm{d}\eta\mathrm{d}\omega. \tag{18}$$

In Eq. (18), $\Omega(x, y, z, t)$ is representative of the dynamic field quantities (displacements, stresses and pore pressures). According to the characteristics of Dirac's delta function, the inverse Fourier transform with respect to ω in Eq. (18) can be performed analytically by replacing ω with $-c\xi$. Consequently, the original triple inverse Fourier transform in Eq. (18) will be reduced to a double integral transform:

$$\Omega(x,y,z,t)=\frac{f_0}{(2\pi)^3}\int_{-\infty}^{\infty}\int_{-\infty}^{\infty}\hat{\hat{\bar{\Omega}}}(\xi,c\xi,\eta,z)\mathrm{e}^{\mathrm{i}\xi(x-ct)}\mathrm{e}^{\mathrm{i}\eta y}\mathrm{d}\xi\mathrm{d}\eta. \tag{19}$$

5 Numerical results and discussion

5.1 Numerical scheme and verification

Note that the solution (Eq. (19)) appears in terms of infinite integrals with a complicated integrand. In view of the complexity of the integrand, it is natural to employ a suitable numerical quadrature scheme to evaluate the integrals. Generally, the branch points and poles of the integrand are all complex-valued with a negative imaginary part if material damping (i.e., complex λ and μ) is considered. Therefore, the real ξ- and η-axis are free from any singularities. In this study, the fast Fourier transform (FFT) method is used to perform the inverse Fourier transform (Sneddon, 1951). To avoid distortion of the results, the integrals must be truncated at sufficiently high values. In addition, the mesh of the calculated integrand must be fine enough to represent well the details of the integrand. According to Cai *et al.* (2007), an FFT algorithm over a grid of 2048×2048 points with a range of $-16\ \mathrm{m}^{-1}\leq\xi\leq16\ \mathrm{m}^{-1}$

and -16 m$^{-1}\leq\eta\leq16$ m^{-1} satisfies both of these requirements.

When h_1=0, as described above, the present model is reduced to a homogeneous saturated half-space. Cai *et al.* (2007) investigated the dynamic response of a homogeneous saturated half-space under a distributed rectangular moving load. For the purpose of verification, Fig. 2 presents a comparison of numerical solutions for non-dimensional displacement w_z^* obtained from the present analysis for the limiting case of a homogeneous saturated half-space (i.e., h_1=0) with those based on Cai *et al.* (2007). The parameters in this example were chosen as follows: μ=1.0×10^7 N/m^2, ν=0.35, M=2.45×10^9 N/m^2, a=1 m, b=0.5 m, Q=120 kN, n=0.4, ρ_s=1816 kg/m^3, ρ_f=1.0×10^3 kg/m^3, α=1 and x_t=$x-ct$. It is clear from Fig. 2 that the two solutions are in good agreement for this reduced example.

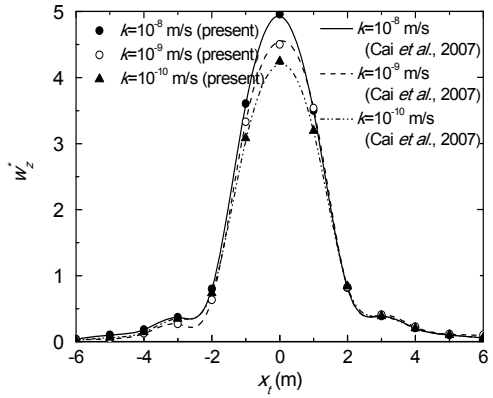

Fig. 2 Comparison of present results with those of Cai *et al.* (2007)

5.2 Numerical results

The numerical results of this section were obtained on the basis of the material parameters given in Table 1 and Table 2. The material damping can be taken into account through the use of complex Lame constants, i.e., $\lambda^*=\lambda(1+\mathrm{i}\delta)$ and $\mu^*=\mu(1+\mathrm{i}\delta)$, where δ denotes the hysteretic damping ratio. The main physical quantities of interest in this investigation are the vertical displacement of the solid u_z and the pore fluid pressure p. u_z and p are normalized as

$$u_z^*=\frac{\mu u_z}{2f_0a},\quad p^*=\frac{p}{f_0}.$$

Table 1 Material parameters of the overlying elastic layer

Parameter	Value
Shear modulus μ^e (N/m^2)	2×10^7
Poisson's ratio ν^e	0.35
Hysteretic damping ratio δ^e	0.1
Material density ρ^e (kg/m^3)	1090
Thickness of the overlying elastic layer h_1 (m)	0–3
Load length 2a (m)	2
Load width 2b (m)	1

Table 2 Material parameters of the underlying saturated half-space

Parameter	Value
Shear modulus μ (N/m^2)	2×10^7
Poisson's ratio ν	0.35
Hysteretic damping ratio δ	0.1
Solid density ρ_s (kg/m^3)	1816
Water density ρ_f (kg/m^3)	1000
Porosity n	0.4
Permeability k (m^3·s/kg)	1.0×10^{-11}–1.0×10^{-6}
Bulk modulus of the fluid M (N/m^2)	2.45×10^9
Compressibility of the solid particle α	0.97

5.2.1 Influence of the drained or undrained free surface on the dynamic response

As discussed above, the solutions for a homogeneous saturated half-space can be easily obtained by assuming h_1=0. In this circumstance, the permeability conditions at the interface (i.e., drained or undrained interface) reduce to the permeability conditions at the free surface of the homogeneous saturated half-space (i.e., the drained or undrained free surface). In this section, we will study the influence of the permeability of the free surface on the nondimensional vertical displacement and pore fluid pressure under the moving load. The observation point is located at (160 m, 0, 0) and the velocity is c=20 m/s.

Fig. 3a shows the variation of nondimensional vertical displacement with time t. It is clear that the maximum displacement occurs at time t=8 s (t=160 m/20 m/s) and the response is not quite symmetric with respect to the plane of the observation due to the presence of damping. The displacement increases for more permeable soil material since dissipative forces are inversely proportional to permeability. The effect of assuming drained or undrained conditions at the free surface is most obvious when

k=5×10^{-7} m^3·s/kg, while for the cases k=1×10^{-9} and k=1×10^{-6} m^3·s/kg, this effect is small. The variation of the maximum displacement (t=8 s) of the observation point with permeability k is illustrated in Fig. 3b. For the two boundary conditions, the displacement shows almost no difference when the permeability is low (k=1×10^{-11}–1×10^{-9} m^3·s/kg), while for more permeable soil material (k=1×10^{-9}–1×10^{-7} m^3·s/kg), the displacement of the drained half-space is obviously larger than that of the undrained half-space. However, with a further increase in permeability (k=1×10^{-7}–1×10^{-6} m^3·s/kg), the value difference derived from the two boundary conditions becomes small again. The case of c=80 m/s is also given in Fig. 3b. As expected, the displacement amplitude of c=80 m/s is larger than that of c=20 m/s. Furthermore, the effect of the drained or undrained free surface is very similar for the two velocities considered.

The effect of the drained or undrained free surface on the nondimensional pore fluid pressure generated by the moving load at the point of interest (160 m, 0, 0) is shown in Figs. 4a and 4b for a specific value of load velocity in each figure. Increasing permeability reduces considerably the fluid pressure for an undrained half-space for a load moving at low speed (c=20 m/s). Because 0<p^*<1, we know that the applied moving load is carried by both the solid and fluid constituents at the undrained free surface. In the case of a drained half-space, the pressure at the free surface is zero everywhere and the moving load is carried completely by the solid skeleton, as expected. From Fig. 4b (c=80 m/s), it can be seen that the nondimensional fluid pressure is close to 1 for an undrained half-space when k=1×10^{-9} m^3·s/kg, which means that almost all the moving load is carried by the pore fluid at this low permeability.

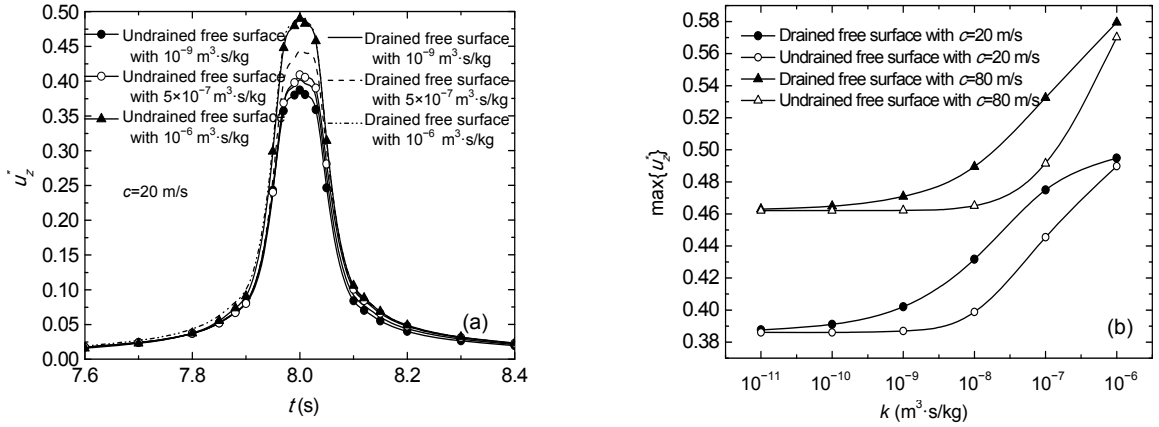

Fig. 3 The nondimensional vertical displacement for the point (160 m, 0, 0) due to a moving rectangular load with different permeability and boundary conditions. (a) u_z^* with time t; (b)max$\{u_z^*\}$ with permeability k

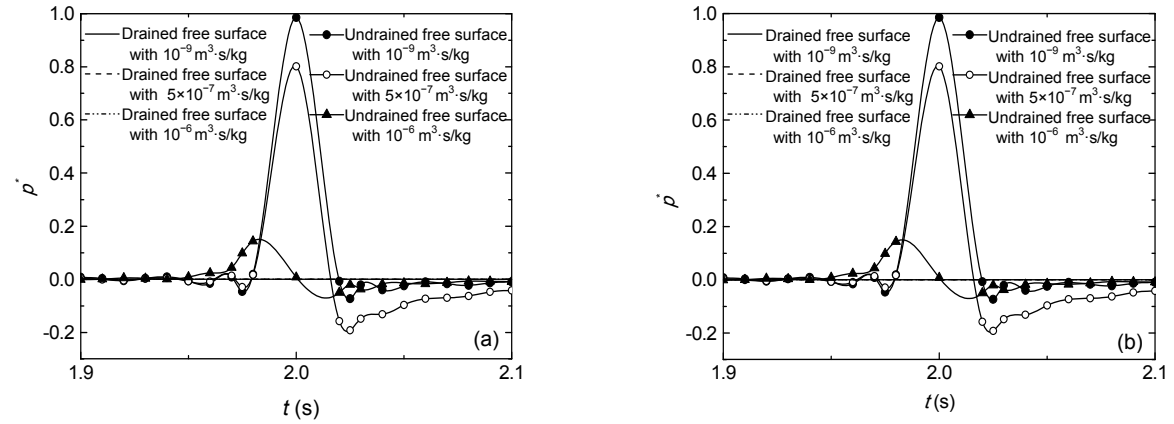

Fig. 4 The nondimensional pore fluid pressure for the point (160 m, 0, 0) due to a moving rectangular load with different permeability and boundary conditions. (a) c=20 m/s; (b) c=80 m/s

Fig. 5a shows the nondimensional vertical displacement with depth z due to a moving load. The maximum displacement appears at z=0 and then diminishes rapidly as the depth increases. As discussed above, the influence of the permeability of the free surface (i.e., a drained or undrained free surface) on the displacement is most obvious when k=5×10^{-7} m^3·s/kg. Nevertheless, as the depth increases, this influence weakens. In addition, the maximum pore fluid pressure difference derived from the drained or undrained boundary exists only near the free surface (0–1 m) (Fig. 5b).

5.2.2 Effect of the overlying dry layer on the dynamic response

In this section, a saturated half-space with an overlying dry layer is considered. The skeletal material below the saturation depth is taken to be the same as that of the upper dry layer (Table 1). Results from this problem (Fig. 6a) indicate that the maximum displacement increases obviously when h_1 changes from 0 to 1.5 m (h_1=0 corresponds to the case of a homogeneous saturated half-space). Note that Fig. 6a relates only to the case of a drained interface with k=1×10^{-9} m^3·s/kg. The variation in the maximum displacement (when t=8 s) of the observation point for the other cases is illustrated in Fig. 6b. For material with k=1×10^{-9} m^3·s/kg and k=5×10^{-7} m^3·s/kg, the maximum displacement is sensitive to the change in the upper dry layer's thickness h_1. However, this sensitivity is limited only to small values of h_1 (0–1.5 m). With a further increase in h_1, the displacement gradually reaches a constant value. For a more permeable soil (k=1×10^{-6} m^3·s/kg), the dry layer has almost no impact on the displacement response. This is because with high permeability, the coupling effect

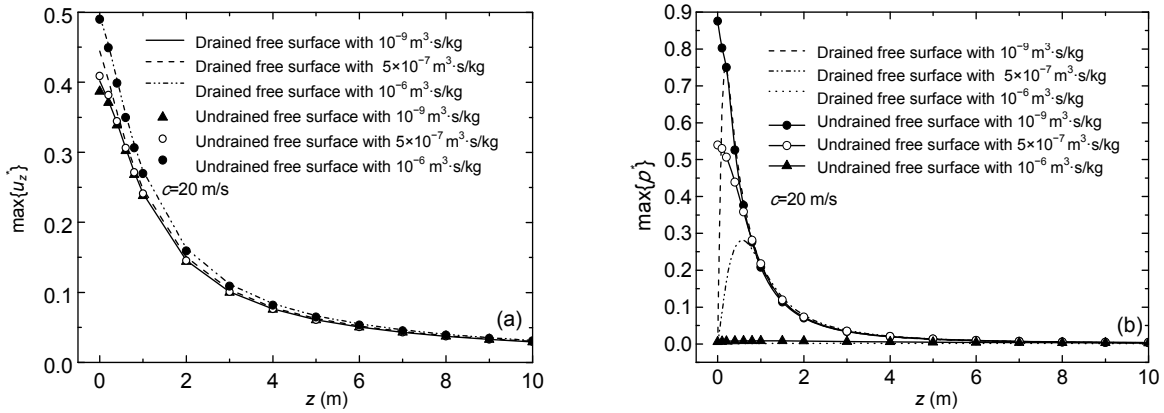

Fig. 5 The nondimensional vertical displacement and pore fluid pressure at depth z due to a moving rectangular load
(a) max$\{u_z^*\}$; (b) max$\{p^*\}$

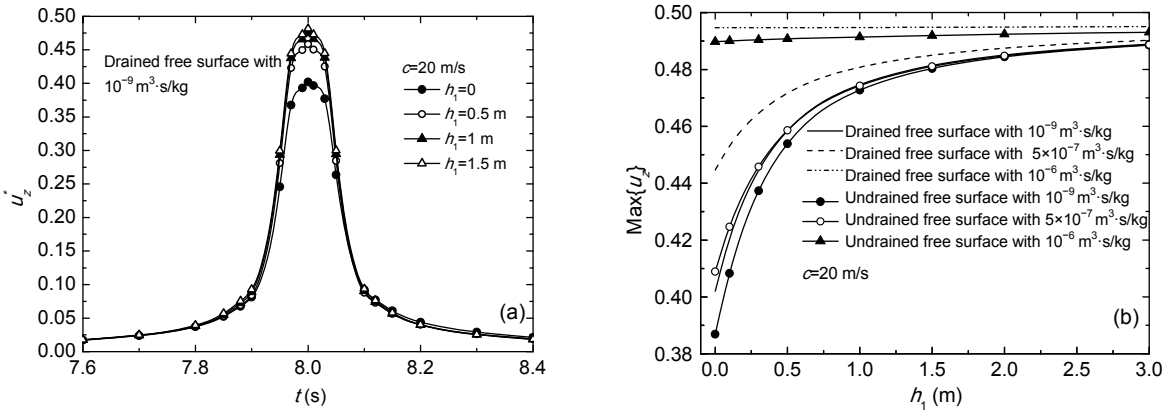

Fig. 6 The nondimensional vertical displacement of the point (160 m, 0, 0) in a saturated half-space with an overlying dry layer due to a moving rectangular load
(a) u_z^* with time t; (b) max$\{u_z^*\}$ with an upper dry layer of thickness h_1

produced by the motions of the solid and fluid is limited. Thus, the underlying saturated soil exhibits behavior similar to that of the upper dry layer in vertical displacement.

6 Conclusions

In this paper, the dynamic response of a saturated half-space with an overlying dry layer generated by a moving rectangular load is presented. Numerical results in time-space domain are evaluated using an FFT algorithm. The following conclusions can be drawn from the numerical studies:

1. The influence of a drained or undrained free surface on the dynamic response is related to the permeability of the soil. For a soil with high or low permeability, the influence is small for the problem considered, while for a soil with moderate permeability, the influence becomes more obvious. Moreover, the effect due to a drained or undrained boundary exists only near the free surface.

2. The effect of the overlying dry layer is associated with the thickness (h_1) of the layer. When the value of h_1 is small, the overlying dry layer has an obvious impact on the dynamic response, and the difference between a drained and undrained interface can be pronounced, depending on the permeability of the underlying saturated half-space. However, with a further increase in h_1, the impact weakens.

References

Biot, M.A., 1956. Theory of propagation of elastic waves in a fluid-saturated porous solid. I. Low-frequency range. *The Journal of the Acoustical Society of America*, **28**(2): 168-178. [doi:10.1121/1.1908239]

Biot, M.A., 1962. Mechanics of deformation and acoustic propagation in porous media. *Journal of Applied Physics*, **33**(4):1482-1498. [doi:10.1063/1.1728759]

Bo, J., 2004. Dynamic responses of a poroelastic half space generated by high speed load. *Chinese Quarterly of Mechanics*, **25**(2):168-174 (in Chinese).

Burke, M., Kingsbury, H.B., 1984. Response of poroelastic layers to moving loads. *International Journal of Solids and Structures*, **20**(5):499-511.

Cai, Y., Sun, H., Xu, C., 2007. Steady state responses of poroelastic half-space soil medium to a moving rectangular load. *International Journal of Solids and Structures*, **44**(22-23):7183-7196. [doi:10.1016/j.ijsolstr.2007.04.006]

Cole, J., Huth, J., 1958. Stress produced in a half-space by moving loads. *Journal of Applied Mechanics*, **25**(2): 433-436.

Eason, G., 1965. The stresses produced in a semi-infinite solid by a moving surface force. *International Journal of Engineering Science*, **2**(6):581-609. [doi:10.1016/0020-7225(65)90038-8]

Hung, H.H., Yang, Y.B., 2001. Elastic waves in visco-elastic half-space generated by various vehicle loads. *Soil Dynamics and Earthquake Engineering*, **21**(1):1-17. [doi:10.1016/S0267-7261(00)00078-6]

Jin, B., Yue, Z.Q., Tham, L.G., 2004. Stresses and excess pore pressure induced in saturated poroelastic halfspace by moving line load. *Soil Dynamics and Earthquake Engineering*, **24**(1):25-33. [doi:10.1016/j.soildyn.2003.09.004]

Lefeuve-Mesgouez, G., Mesgouez, A., 2008. Ground vibration due to a high-speed moving harmonic rectangular load on a poroviscoelastic half-space. *International Journal of Solids and Structures*, **45**(11-12):3353-3374. [doi:10.1016/j.ijsolstr.2008.01.026]

Lu, J.F., Jeng, D.S., 2007. A half-space saturated poro-elastic medium subjected to a moving point load. *International Journal of Solids and Structures*, **44**(2):573-586. [doi:10.1016/j.ijsolstr.2006.05.020]

Siddharthan, R., Zafir, Z., Norris, G.M., 1993. Moving load response of layered soil. I: Formulation. *Journal of Engineering Mechanics*, **119**(10):2052-2071. [doi:10.1061/(ASCE)0733-9399(1993)119:10(2052)]

Sneddon, I.N., 1951. Fourier Transforms. McGraw-Hill Book Company, New York.

Sneddon, I.N., 1952. The stress produced by a pulse of pressure moving along the surface of a semi-infinite solid. *Rendiconti del Circolo Matematico di Palermo*, **1**(1): 57-62. [doi:10.1007/BF02843720]

Theodorakopoulos, D.D., 2003. Dynamic analysis of a poroelastic half-plane soil medium under moving loads. *Soil Dynamics and Earthquake Engineering*, **23**(7):521-533. [doi:10.1016/S0267-7261(03)00074-5]

Xu, B., Lu, J.F., Wang, J.H., 2008. Dynamic response of a layered water-saturated half space to a moving load. *Computers and Geotechnics*, **35**(1):1-10. [doi:10.1016/j.compgeo.2007.03.005]